

QUALITY FACTOR OF S-WAVE IN NW IRAN

Tayebeh HEYDARI

*Institute for Advanced Studies in Basic Sciences (IASBS)Zanjan, Iran
heydari@iasbs.ac.ir*

Farhad SOBOUTI

*Institute for Advanced Studies in Basic Sciences (IASBS)Zanjan, Iran
farhads@iasbs.ac.ir*

Khalil MOTAGHI

*Institute for Advanced Studies in Basic Sciences (IASBS)Zanjan, Iran
kmotaghi@iasbs.ac.ir*

Keywords: Quality Factor, Shear Wave, Spectral Amplitude, Attenuation, NW Iran

ABSTRACT

In this paper, we estimated shear wave quality factor in NW Iran using data recorded at IRSC stations in the period 1996 - 2006. We used the spectral amplitude ratio method in the frequency range of 1.5-15.5 Hz, to calculate Q_d . We obtained a power law relation of the form $Q_d = 94 \pm 3f^{0.6 \pm 0.1}$ for NW Iran.

INTRODUCION

Estimation of seismic risk in a region requires an understanding of the attenuation of strong ground motion. Seismic waves attenuate as a result of the different processes such as scattering due to heterogeneities, intrinsic absorption due to anelasticities and geometrical spreading in the earth. Northwest Iran is an active tectonic region and affected by intensive magmatism and volcanism in the Mesozoic and the Cenozoic. Various seismological and petrological studies have inferred elevated temperatures in the crust and the mantle, and a relatively thin lithosphere in this region. As a result of this history of high deformation rates, the NW Iran might be a region of high seismic attenuation. In this study, we investigate attenuation of shear waves in NW Iran using local events recorded at the stations of IRSC. For this purpose, 132 waveforms recorded by eight short period stations of the Tabriz network (TBZ, BST, AZR, HRS, HSH, SHB, MRD, SRB) from 1996 to 2006 have been analysed. Fig. 1 shows stations, events and ray coverage used in this study. We used the method of spectral amplitude ratios versus distance (Tsujiura, 1966) to obtain the frequency dependence of Q_d over the study region.

DATA ANALYSIS

We calculated spectral amplitudes on the transverse component (T) in a shear wave window containing 90% of the total shear wave energy. Fig. 2 shows an example of the records and Fig. 3 shows an example shear wave window. A noise window after P wave arrival was also selected for the purpose of calculating signal-to-noise ratio. We analysed waveforms with signal to noise ratio greater than 2. To avoid

Gibbs' phenomenon, we applied a 5% cosine-taper to the beginning and the end of the time series of the signal window and the spectrum was calculated using an FFT.

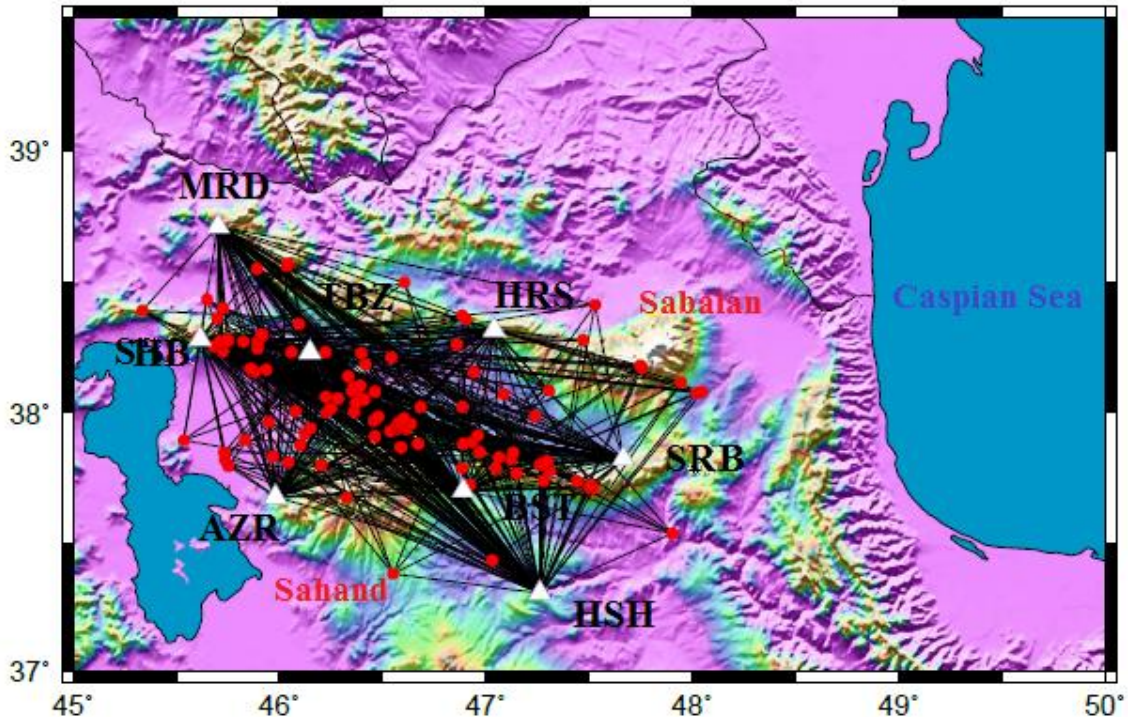


Figure 1. Map showing the seismic network and the ray coverage used in this study. 132 events (red circles) recorded at eight stations (white triangles) have been analysed.

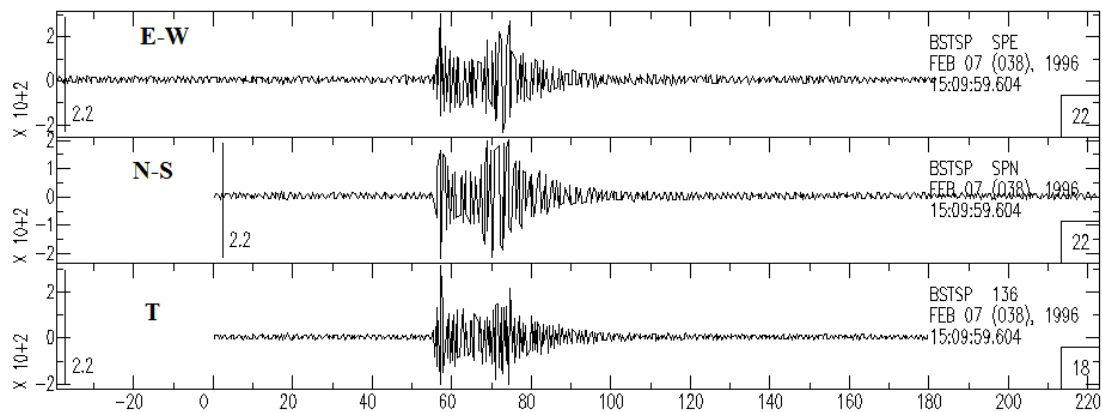


Figure 2. Example of the seismic record (E-W) & (N-S) component and transverse component (T) for one station.

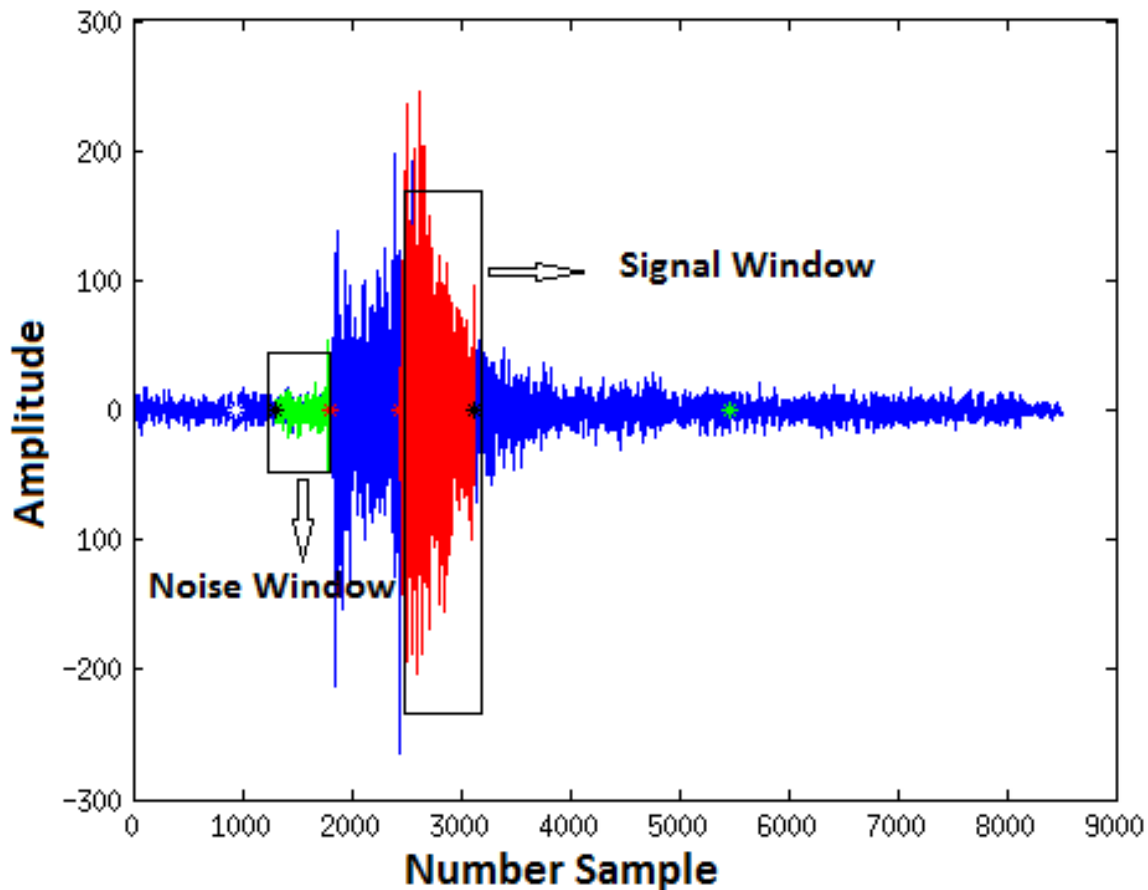


Figure 3. An example seismogram for an event that shows the S window as defined by the 90% energy criterion (red) and a noise window 10 second long after the arrival time of P wave (green).

The ratio of amplitude at frequency f_1 to amplitude at frequency f_2 as a function of shear wave travel time is given by (Tsujiura, 1966):

$$\ln [A_b (f_1)/A_b (f_2)] = \ln [A_0 (f_1)/A_0 (f_2)] + \ln [R (f_1)/R (f_2)] - \pi (f_1 - f_2) t / Q_d \quad (1)$$

$$\text{Slope} = - \pi (f_1 - f_2) / Q_d$$

Where A_b is the amplitude of shear wave at two frequencies f_1 and f_2 , t is the travel time of the shear wave, A_0 is the spectral amplitude of the source at f_1 and f_2 , and $R (f)$ is the site effect. The ratios of source amplitudes and site effects are assumed constant. Therefore, the above equation is a straight line, and the slope of the line gives Q_d . We assumed that all events had similar source functions, and thus, chose earthquakes with magnitudes between 2 and 4. We studied the spectral ratio of horizontal to vertical components ($R (f) = H (f)/V (f)$), to verify that the site response at the stations is flat over the entire frequency band. Our results show that $\ln (H (f)/V (f))$ is near zero in all stations (for example station HRS in Fig. 3), which was expected, since all stations are located on hard rock (Atkinson, 1993). Therefore we removed the site effect term from Eq. 1. We calculated the logarithm of the spectral amplitude ratios at different frequencies ($f_1=1$ Hz and $f_2 = 1.26, 1.58, 2, 2.51, 3.16, 3.98, 5.01, 6.31, 7.94, 10, 12.59, 15.85$ Hz) versus shear wave travel time, and fitted a straight line to the data, and from the slope of that line we computed Q_d . Fig. 5 shows the results of line fitting for one event recorded at five stations.

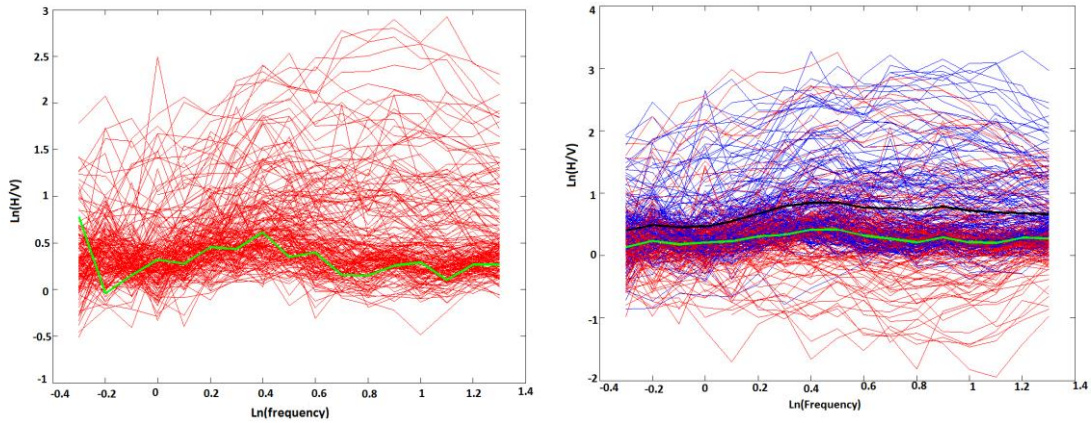


Figure 4. Plot of $\ln(H(f)/V(f))$ versus $\ln(\text{central frequency})$ at station HRS. Right: blue lines are plots of (E-W)/Z (black line is the average), red lines are plots of (N-S)/Z (green line is the average); Left: red lines are plots of $\{(E-W)^2 + (N-S)^2/2\}^{1/2}$ and green line is the average.

Fig. 6 shows variation of Q_d with frequency for all ray paths used. Table 1 and Fig. 7 show the variation of mean Q_d with frequency. In calculation of the mean values, the data with correlation coefficient less than 0.1 are discarded. The frequency dependence is strong up to 5 Hz, after which Q_d increases with a slower rate. By fitting the following formula to the mean values;

$$\text{Log } Q = \text{Log } Q_0 + n \text{Log } f \tag{2}$$

Where Q_0 is Q at 1 Hz, and n is frequency parameter (Sing & Herman, 1983). We obtained;
 $Q_d = 94 \pm 3f^{0.6 \pm 0.1}$.

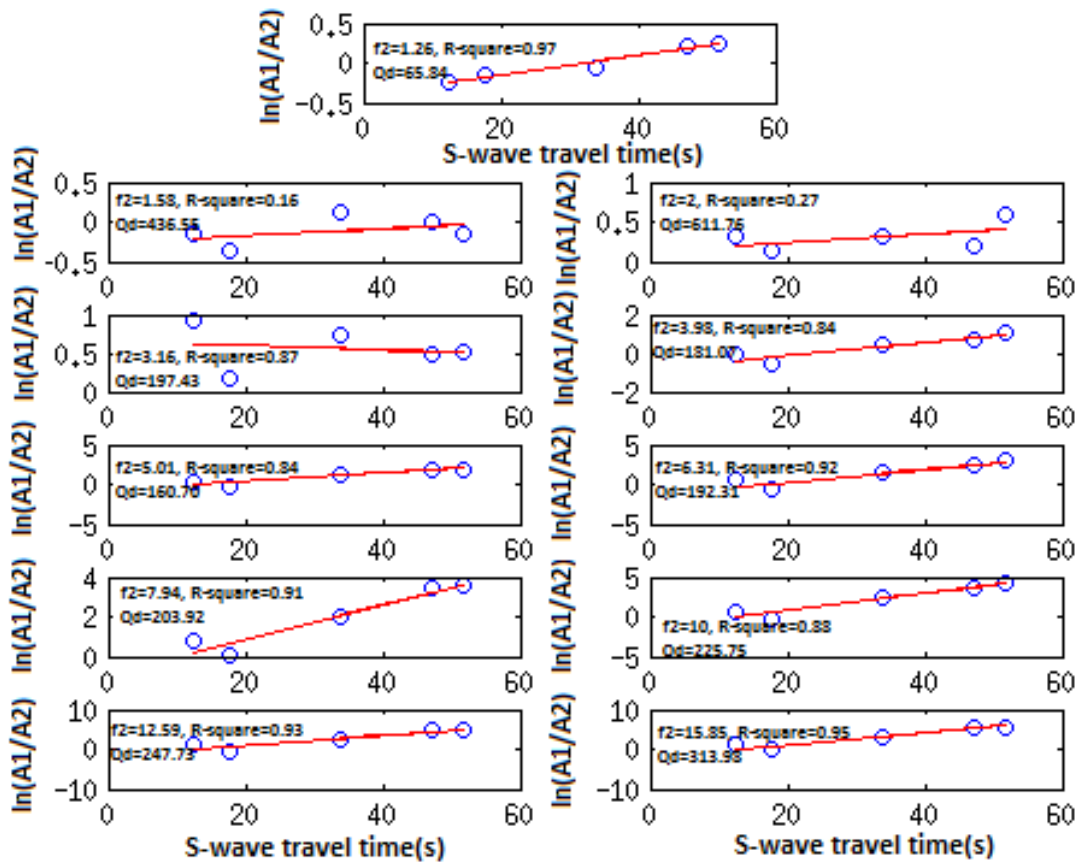


Figure 5. Plots of $\text{Ln} [A_b(f_1)/A_b(f_2)]$ versus travel time at each of the 11 central frequencies for one event.



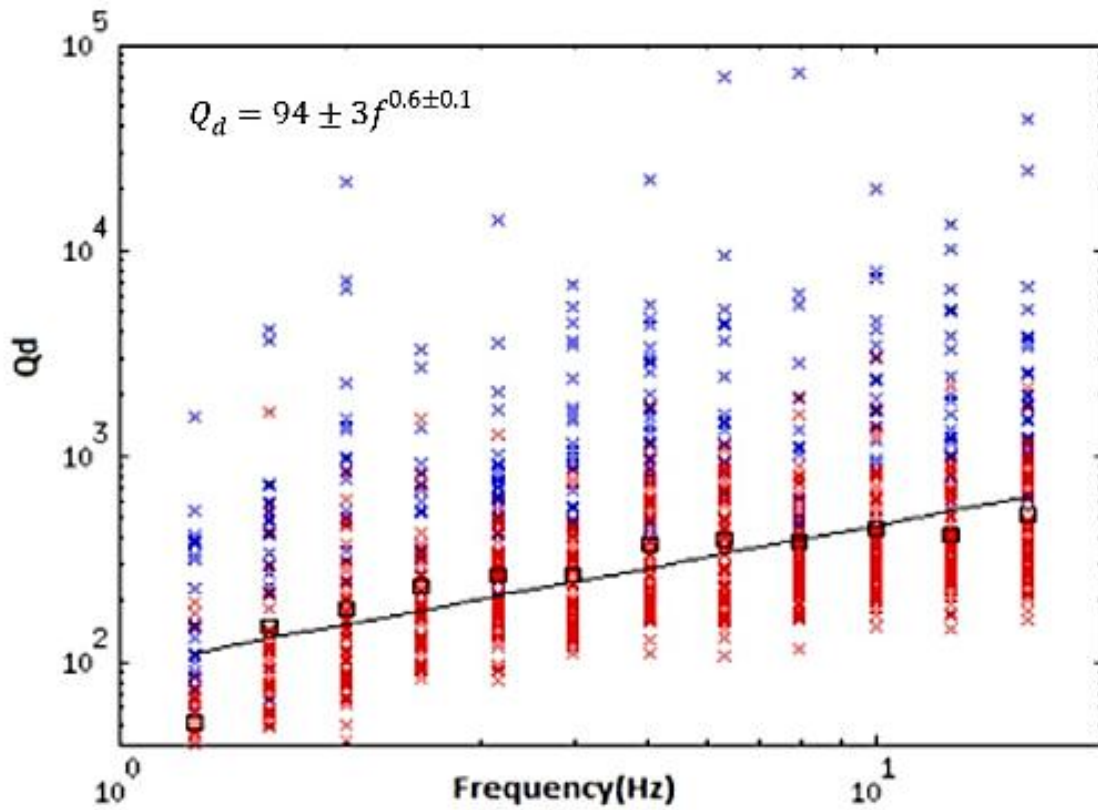


Figure 6. Q_d versus central frequencies ($f=1.26, 1.58, 2, 2.51, 3.16, 3.98, 5.01, 6.31, 7.94, 10, 12.59, 15.85$ Hz) in natural log-log scale. Blue symbols are data not used in calculating the mean values.

Table 1. Mean Q_d values for the twelve central frequencies.

No.	Frequency(Hz)	Q_d
1	1.26	50 ± 38
2	1.58	147 ± 240
3	2.00	181 ± 145
4	2.51	235 ± 218
5	3.16	261 ± 176
6	3.98	261 ± 149
7	5.01	378 ± 283
8	6.31	393 ± 244
9	7.94	382 ± 280
10	10.00	444 ± 389
11	12.59	417 ± 264
12	15.85	512 ± 324

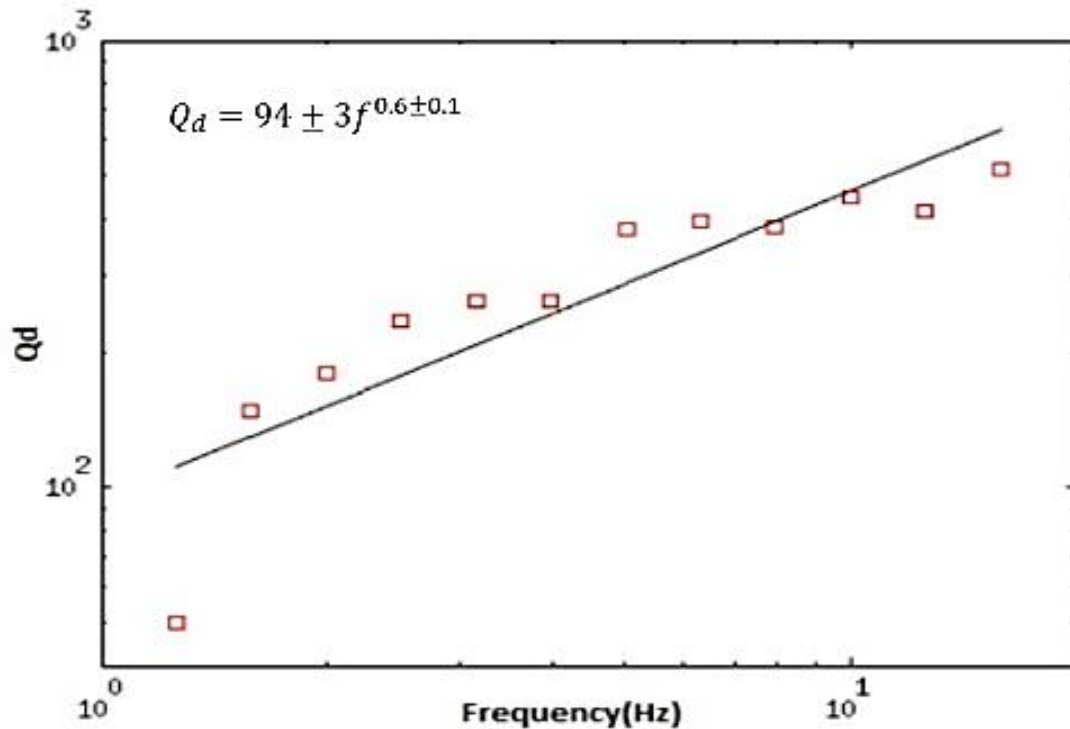


Figure 7. Q_d versus central frequencies ($f=1.26, 1.58, 2, 2.51, 3.16, 3.98, 5.01, 6.31, 7.94, 10, 12.59, 15.85$) fit by a regression line.

CONCLUSIONS

We have obtained low values for Q_d at different frequencies. The mean value of Q_d at 1 Hz for the entire region is 94 ± 3 ; this value is relevant to regions of high seismicity and intense tectonic activity. In comparison, Ma'hood et al. (2009) have obtained values of about 50 in east central Iran where major strike-slip faults and high rate of seismicity shape the tectonic characteristics of that region. The North Tabriz Fault is the dominant tectonic structure in our region of study, whose broad zone of deformation has a major effect on the quality of wave propagation in its vicinity. Furthermore NW Iran is a region of significant geothermal activity and anomalously high crustal temperatures. These geothermal activities result in smaller values for quality factor and higher attenuation of seismic waves.

REFERENCES

- Atkinson M and Mereu R (1992) The Shape of Ground Motion Attenuation Curves in South Eastern Canada, *Bul. Seis. Soc. Am.*, 82(5): 2014-2031
- Atkinson G (1993) Notes on Ground Motion Parameters for Eastern North America Duration and H/V Ratio, *Bul. Seis. Soc. Am.*, 83(2): 587-596
- Mahood M, Hamzeloo H and Doloei GJ (2009) Attenuation of High Frequency P and S wave in the Crust of the East Central Iran, *Geophysics. J. Int.*, 10: 1111-1365
- Mukhopadhyay S and Tyagi C (2008) Variation of Intrinsic and Scattering Attenuation with Depth in NW Himalayas, *Geophysics. J. Int.*, 172: 1055-1065
- Tsujiura M (1966) Frequency Analysis of the Seismic Waves, *Bull. Earth. Res. Inst. Tokyo Univ.*, 44:873-891

